Bioorganic & Medicinal Chemistry 19 (2011) 1349–1360

Contents lists available at ScienceDirect

Bioorganic & Medicinal Chemistry

journal homepage: www.elsevier.com/locate/bmc

Pharmacophore models based studies on the affinity and selectivity toward 5-HT$_{1A}$ with reference to α_1-adrenergic receptors among arylpiperazine derivatives of phenytoin

Jadwiga Handzlik [a], Ewa Szymańska [a], Krystyna Nędza [b], Monika Kubacka [c], Agata Siwek [d], Szczepan Mogilski [c], Jarosław Handzlik [e], Barbara Filipek [c], Katarzyna Kieć-Kononowicz [a,*]

[a] Department of Technology and Biotechnology of Drugs, Jagiellonian University Medical College, Medyczna 9, PL 30-688 Kraków, Poland
[b] Department of Medicinal Chemistry Institute of Pharmacology, Polish Academy of Sciences, Smetna 12, PL 31-343 Kraków, Poland
[c] Department of Pharmacodynamics, Jagiellonian University Medical College, Medyczna 9, PL 30-688 Kraków, Poland
[d] Department of Pharmacobiology, Jagiellonian University Medical College, Medyczna 9, PL 30-688 Kraków, Poland
[e] Faculty of Chemical Engineering and Technology, Cracow University of Technology, Warszawska 24, PL 31-155 Kraków, Poland

ARTICLE INFO

Article history:
Received 20 March 2010
Revised 17 November 2010
Accepted 20 November 2010
Available online 5 December 2010

Keywords:
Arylpiperazine derivatives
Phenytoin derivatives
5-HT$_{1A}$ receptor
N-Triphenylmethyl protection

ABSTRACT

The study is focused on (2-alkoxy)phenylpiperazine derivatives of 1-(2-hydroxy-3-(4-arylpiperazin-1-yl)propyl)-5,5-diphenylimidazolidine-2,4-dione with alkyl or ester substituents at N3 of hydantoin ring, as well as a new designed and synthesized series of compounds with a free N3H group or N3-acetic acid terminal fragment. The compounds were assessed on their affinity for 5-HT$_{1A}$ and α_1-adrenoceptors and evaluated in functional bioassays for antagonistic properties. Classical molecular mechanics (MMFFs force field, MCMM, MacroModel) and DFT methods (B3LYP functional, Gaussian 0.3) were used to investigate 3D structure of the compounds. SAR analysis was based on two pharmacophore models, the one described by Barbaro et al. for α_1-adenoceptor antagonist and the model of Lepailleur et al. for 5-HT$_{1A}$ receptor ligands. All compounds exhibited significant to moderate affinities for 5-HT$_{1A}$ receptors in nanomolar range (7–610 nM). The highest activity (7 nM) and selectivity (17.38) for 5-HT$_{1A}$ was observed for 1-(3-(4-(2-ethoxyphenyl)piperazin-1-yl)-2-hydroxypropyl)-3-methyl-5,5-diphenylimidazolidine-2,4-dione (**13a**). Among new synthesized compounds 1-(2-hydroxy-3-(4-(2-methoxyphenyl)piperazin-1-yl)propyl)-5,5-diphenylimidazolidine-2,4-dione hydrochloride (**20a**) displayed the highest affinity (16.6 nM) and selectivity (5.72) for α_1-AR.

1. Introduction

Arylpiperazine moiety is a popular chemical fragment that can be found in active compounds with various biological specificities. Many lines of evidence[1–9] have indicated a potential usage of arylpiperazine derivatives in the treatment of circulation diseases,[1–4] CNS failures[4–6] and bacterial infections.[8,9] Arylpiperazine derivatives (Fig. 1), Urapidil (**1**) and Naftopidil (**2**), are known antihypertensive agents. Recently Malawska et al.[1] has described a group of phenylpiperazine derivatives of pyrrolidin-2-one with significant antiarrhythmic and hypotensive activity in primary screening in vivo. Phenylpiperazine derivatives of hydantoin presented in our previous works[2,3] showed antiarrhythmic activity in the adrenaline induced model of arrhythmia and influenced ECG of rats in similar way to that of class Ia and III of Vaughan-Williams classification of antiarrhythmic agents. Hayao et al.[4] obtained phenylpiperazine derivatives of trimethoxybenzoate that displayed sedative and hypotensive properties. Some of them (**7**, **8**) were tested in clinical trials as effective tranquilizers (Fig. 1). Antinociceptive activity of compounds with phenylpiperazine moiety was confirmed by studies of Cesari et al.[5] performed for arylpiperazinylalkylpyridazinones. Especially, arylpiperazine derivatives seem to be an interesting target in the search for antidepressant drugs. So far several phenylpiperazine agents, including Trazodone (**4**), Nefazodone (**5**), Aripiprazole (**3**) or Flesinoxan (**6**) (Fig. 1), achieved pharmaceutical market as psychoactive drugs useful in major depressive disorder.[6] For *N*-phenylpiperazine dioxolones hypocholesterolemic activity was found.[7] Among arylpiperazines activity against gram-positive bacteria[8] or efflux pump inhibitors,[9] promising in therapy of infectious diseases, has been confirmed as well.

The most important therapeutic potency of arylpiperazine derivatives is in close connection to their interactions with GPCRs (G-protein coupled receptors) including α-adrenergic,[10,11] 5-HT or dopamine receptors.[12,13] The competition in binding towards several GPCRs-members is a serious factor that significantly limits selectivity of pharmacological properties of active arylpiperazine

* Corresponding author. Tel.: +48 012 620 55 81; fax: +48 012 620 55 96.
E-mail address: mfkonono@cyf-kr.edu.pl (K. Kieć-Kononowicz).

0968-0896/$ - see front matter © 2010 Elsevier Ltd. All rights reserved.
doi:10.1016/j.bmc.2010.11.051

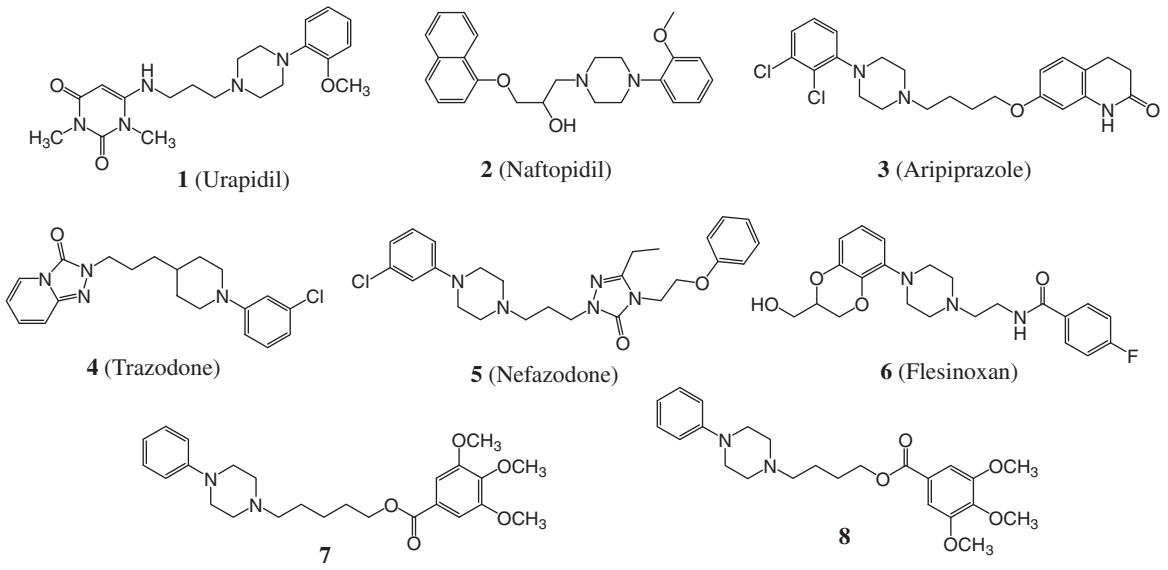

Figure 1. Structure of arylpiperazine derivatives with various therapeutic potency; compounds useful in therapy of hypertension (**1**, **2**), anti-depressant drugs (**3**–**6**), tranquilizers under clinical trials (**7**, **8**).

derivatives and their ability for therapeutic usage. A main problem is a weak selectivity between 5-HT_{1A} and α_1-adrenoceptors. In last years pharmacophore models created for active compounds and describing the structural features responsible for binding properties at selected GPCRs were reported. In case of α_1-adrenoceptor antagonists, the early pharmacophore model, elaborated by De Marinis,[14] proposed three following important features: aromatic area, basic nitrogen and semi-polar or internal lipophilic area. Further evolutions of pharmacophore study were given by De Benedetti's model[15] (Fig. 2), models of Bremner et al. that respected α_1-adrenoceptor subtypes selectivity[16,17] and model of Barbaro,[18] especially adequate for arylpiperazine derivatives (Fig. 3). Pharmacophore models of serotonin receptors ligands have been created for above thirty years.[13,19] The basic model, discriminating agonistic and antagonistic properties at 5-HT_{1A}, is known as Hilbert's model[20] and postulates two distances crucial for interactions with the receptor. During the next twenty years a number of pharmacophore models of 5-HT_{1A} ligands have been elaborated,[21–26] including simple quantitative models developed by

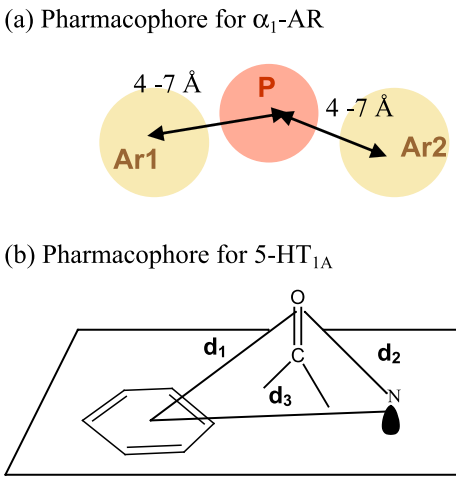

Figure 2. Pharmacophore models. (a) De Benedetti's model for α_1-adrenoceptor antagonist: P (red), protonated nitrogen; Ar1, Ar2 (dark yellow) aromatic systems; distances P-Ar1 and P-Ar2 should be in range of 4–7 Å.[15] (b) Chilmonczyk's model for buspiron-like 5-HT_{1A} receptor ligands; the three centres from a triangle with sides defined by: d_1 = 7.07 Å, d_2 = 4.30 Å, d_3 = 4.88 Å distances.[13]

Mokrosz et al.[23] and Chilmonczyk et al.[25] (Fig. 2) and a modern model of Lepailleur et al.,[26] elaborated by use of CATALYST, comparable to Barbaro's model for α_1-AR antagonists (Fig. 3).

Our previous works[2,27] described synthesis and affinity of N1-arylpiperazine Phenytoin (**23**) derivatives for both α_1- and α_2-adrenoceptors.[27] Results of SAR studies supported by molecular modelling calculation confirmed a close relationship between a range of affinity for α_1-adrenoceptor and five pharmacophore features of Barbaro's model (Fig. 3). In fact, the 2-alkoxyphenylpiperazine derivatives fitting two hydrophobic areas (HY1, HY2) showed the highest activity.[27] Results indicated that a kind of a substituent at N3 of the hydantoin ring, a feature not included in Barbaro's model, influenced α_1-affinity and α_2/α_1 selectivity among the described arylpiperazines. As this influence was unclear, the further investigation was needed. Basing on this conclusion, the current study is focused on N1-(2-alkoxy)phenylpiperazine derivatives with various substituents at N3 of hydantoin (Table 1), including alkyl (**9a**, **12a**–**14a**), ester moieties (**10a**, **11a**, **15a**–**18a**) as well as a series of new designed and synthesized compounds with free NH group (**19a**–**21a**) or acetic acid terminal fragment (**22a**). The new compounds (**19a**–**22a**) were assessed on their affinity to α_1-adrenoceptors, for their antagonistic properties determination the functional bioassays were performed. For compounds **9a**–**22a**, their affinity to 5-HT_{1A} was evaluated in radioligand binding assays. Selectivity studies concerned α_1/5-HT_{1A} selectivity for all compounds (**9a**–**22a**). The work is focused on the SAR study to resolve two following problems: (i) search for structural parameters responsible for activity and selectivity α_1/5-HT_{1A}, (ii) usefulness of available pharmacophore models to search for selective agents among arylpiperazine derivatives of phenytoin. In this field, molecular modelling by use of the newest calculation methods was performed. SAR analysis was based mainly on two pharmacophore models, created by the comparable calculating methods (CATALYST), described by Barbaro et al.[18] and Lepailleur et al.[26] for α_1-AR and 5-HT_{1A} receptors, respectively (Fig. 3).

2. Results and discussion

2.1. Synthesis

The synthesis of compounds **9a**–**18a** was described previously.[2,27] Compounds **19a**–**21a** were obtained in four-step synthesis,

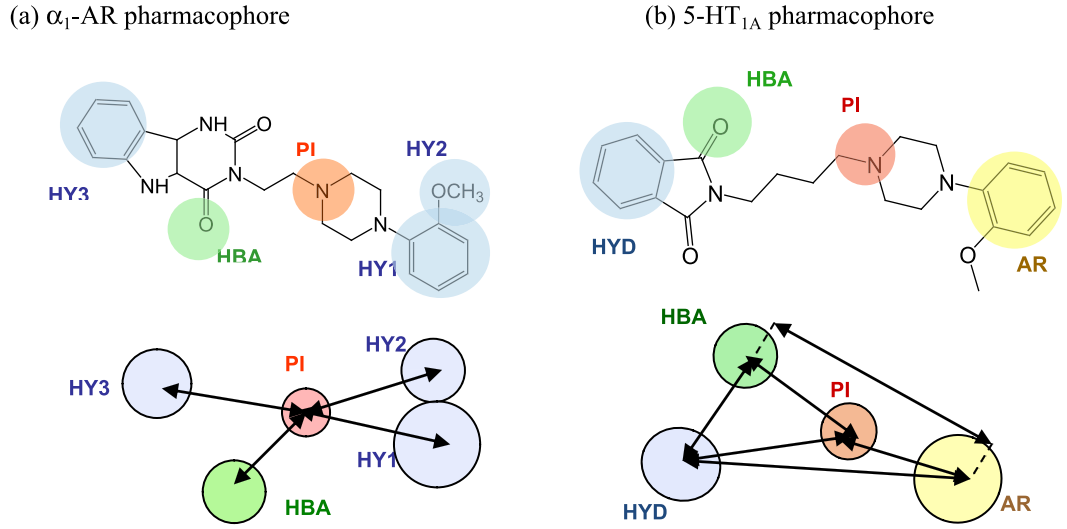

Figure 3. Pharmacophore features of selected GPCR's ligand elaborated by the use of CATALYST. (a) The Barbaro's model of α_1-adrenoceptor antagonist (mapped with a phenylpiperazine antagonist, (3-(2-(4-(2-methoxyphenyl)piperazin-1-yl)ethyl)-4a,5-dihydro-1*H*-pyrimido[5,4-*b*]indole-2,4(3*H*,9b*H*)-dione); PI, positive ionisable centre; HY1-3, three hydrophobic moieties; HBA, hydrogen bound acceptor). Selected distances are crucial for the activity.[18] (b) The 5-HT_{1A} pharmacophore model described by Lepailleur et al. (maped with phenylpiperazine derivatives, NAN-190); PI, positive ionisable centre; HYD, hydrophobic moiety; AR, aromatic ring; HBA, hydrogen bound acceptor. Six selected distances are important for expected activity.[26]

Table 1
Structure and binding properties at 5-HT_{1A} receptors in comparison to α_1-AR for the tested N1-arylpiperazine derivatives of hydantoin **9a**–**22a**

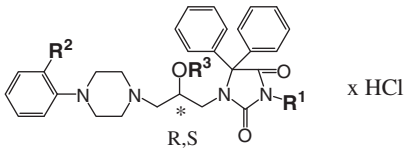

Compounds 9a-22a

Compd	R^1	R^2	R^3	K_s (nM) 5-HT_{1A}	K_i[a] (nM) α_1-AR	Sel α_1/5-HT_{1A}	Antagonist potency pK_B ± SEM
9a	$-C_2H_5$	H	H	610 ± 25	529 ± 9.5	0.86	
10a	$-CH_2COOC_2H_5$	OCH_3	H	88 ± 12	160 ± 21.3	1.82	
11a	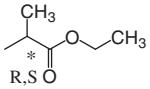	OCH_3	H	30 ± 4	135.7 ± 31.3	4.52	
12a	$-CH_3$	OCH_3	H	22 ± 0.1	160.7 ± 13.6	7.27	
13a	$-CH_3$	OC_2H_5	H	7 ± 1	121.6 ± 14.9	17.37	
14a	$-CH_3$	OC_2H_5	$-COCH_3$	38 ± 0.5	607 ± 74.7	15.97	
15a	$-CH_2COOCH_3$	OCH_3	H	86 ± 13	197.8 ± 25.4	2.29	
16a	$-CH_2COOCH_3$	OC_2H_5	H	37 ± 3	251.6 ± 3.8	6.8	
17a	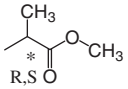	OCH_3	H	104 ± 2	103.9 ± 4.2	1.00	
18a	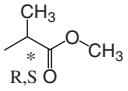	OC_2H_5	H	28 ± 3	167.7 ± 8	5.99	
19a	H	H	H	573 ± 48	731,9 ± 33.2	1.28	–
20a	H	OCH_3	H	95 ± 7	16,6 ± 1.0	0.17	7.79 ± 0.025
21a	H	OC_2H_5	H	83 ± 5	67,4 ± 17.8	0.81	7.44 ± 0.025
22a	$-CH_2COOH$	OCH_3	H	575 ± 0	4800 ± 500	8.35	–
Buspirone				16 ± 3	–		
Prazosin				–	0.24 ± 0.05		

[a] Results for compounds **9a**–**18a** from earlier Ref. 27.

according to Scheme 1. In the first step, 5,5-diphenylhydantoin (**23**) was protected at N3-position giving 5,5-diphenyl-3-tritylimidazolidine-2,4-dione (**24**) by the introduction of a triphenylmethyl (trityl) group using trityl chloride in a diluted solution of methylene chloride in a presence of TEA (triethylamine). In the second step of synthesis, compound **24** was converted into **25** by

two-phase alkylation in a basic condition, similar to that described previously (acetone/K_2CO_3/TEBA).[2,27] The pure oxiran derivative **25** was used in the reaction with respective *ortho*-(un)substituted *N*-phenylpiperazines to give **26**–**28**. The reactions were performed under microwave irradiation in a simple microwave oven. The method was a next modification of microwave-aided reaction described earlier,[2,27] adopted for reactants with higher difference of melting points. Before irradiating, compound **25** with equimolar amount of respective arylpiperazine was carefully dissolved in methylene chloride, then the solvent was evaporated and the residue was irradiated under TLC-control as long as the reaction progress stopped. In the case of trityl derivatives **26**–**28**, the time (7–25 min) and the power of irradiation were higher in comparison to those described for the products **10**–**18**.[2,27] It seems to be connected with high melting point of the starting material (**25**) and a rest of CH_2Cl_2 in reactants-mixture that poorly transmits microwaves as a nonpolar solvent. In contrast to the synthesis of compounds **9**–**18**, compounds **26**–**28** easily crystallized from methanol giving pure white solids with good yield (68–92%). In the last step of synthesis, compounds **26**–**28** were deprotected from the trityl group.

N-Protection was the main problem in the presented synthesis of the target hydantoins possessing an alkyl substituent at N1-position and the free N3-position of the ring, as the nitrogen atom N3 is more susceptible for alkylation. Thus, it was necessary to find a protecting group appropriate for amide nitrogen and selective for N3-position over N1-position. Furthermore, the protecting group had to be stable in basic conditions during the second step of synthesis and easily eliminated at the end of synthesis. In this context, two protecting methods were considered: a method with ethyl chloroformate[28] and the method with triphenylmethyl chloride. In the first one, the protecting group was easily introduced in N3-position giving ethyl 2,5-dioxo-4,4-diphenylimidazolidine-1-carboxylate, but the protection was partly eliminated during the alkylation in two phase-transfer catalytic conditions in the presence of potassium carbonate and benzyltriethylammonium chloride (TEBA) to give a number of by-products. On the contrary, the *N*-trityl protection was stable during all synthesis steps, but it was hard to remove it to obtain the target products (**19**–**21**). Compounds **26**–**28** were stable in the basic conditions and resistant to deprotection by the long-term heating in the concentrated HCl (38%) yielding hydrochlorides of 1-(2-hydroxy-3-(4-arylpiperazin-1-yl)propyl)-5,5-diphenyl-3-tritylimidazolidine-2,4-diones.

The successful deprotection was accomplished using long-term stirring of compounds **26**–**28** dissolved in methylene chloride with the concentrated trifluoroacetic acid (TFA). The final products were converted into hydrochloric forms **19a**–**21a** with gaseous HCl and precipitated from methanol (**19a**) or the mixture of methanol with diethyl ether (**20a**, **21a**).

Synthesis of N3-acetic acid derivative **22a** (Scheme 1) was performed as a basic hydrolysis of the corresponding ester (**10**), synthesized within our previous work.[2] The crude product of the

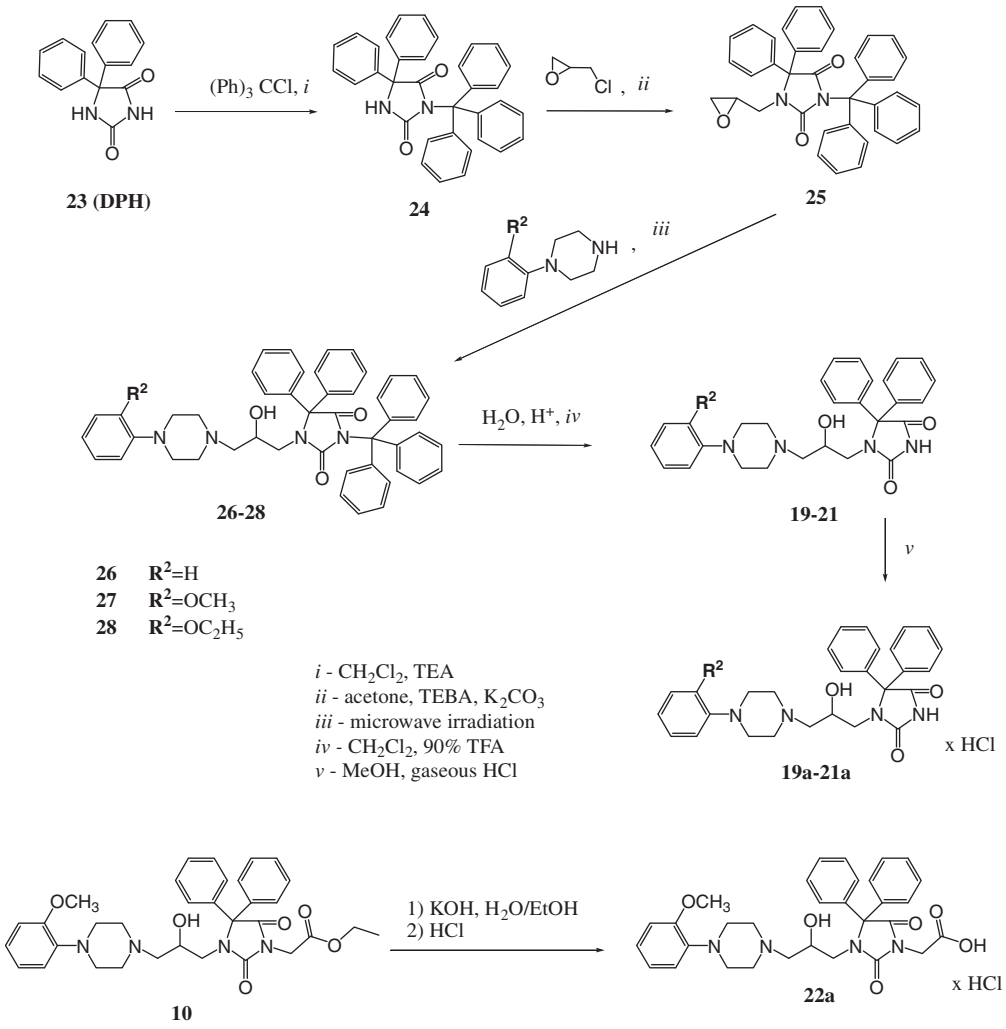

Scheme 1. Synthesis of compounds **19a**–**22a**.

hydrolysis, dissolved in absolute ethanol, was converted into hydrochloride **22a** by the use of gaseous HCl.

Compounds **9a**–**22a** possessing one or two chiral centres were obtained and tested as racemates.

2.2. Pharmacology

2.2.1. Radioligand binding study

Affinity for 5-HT_{1A} receptors was determined using [^{3}H] 8-OH DPAT as a radioligand, based on the screening protocol described earlier.[29] The ligands affinities expressed as estimated Ks values (nM) are shown in Table 1.

Affinity for α_1-adrenoceptors of compounds **9a**–**18a** was evaluated previously.[27] Compounds **19a**–**22a** were tested for their in vitro affinity for α_1-adrenoceptors on rat cerebral cortex by the radioligand binding assays using [^{3}H]-prazosin as a specific radioligand. The affinities described by K_i values (nM) are shown in Table 1. Selectivity toward 5-HT_{1A} over α_1-AR was calculated as $K_{i\alpha1}/K_{s5HT1A}$. For 5-HT_{1A} receptors compounds **9a**–**22a** showed affinity within the range of 7–610 nM, whereas the affinity values for α_1-AR of new compounds (**19a**–**22a**) were included in the wide range of 16.6–4800 nM.

In the case of affinity for 5-HT_{1A}, three groups of the activity may be seen: (I) the group of potent ligands with affinities in range of 7–38 nM (**11a**–**14a**, **16a**, **18a**), (II) the group of active ligands with affinities in range of 83–104 nM (**10a**, **15a**, **17a**, **20a**, **21a**) and (III) the compounds with moderate affinities in range of 573–610 nM (**9a**, **19a**, **22a**).

2.2.2. Functional bioassays results

The antagonist activity of compounds **20a** and **21a** toward α_1-adrenoceptors present in rat aorta from adult Wistar rats was assessed by inhibition of phenylephrine induced contractions. The investigated compounds shifted the phenylephrine response to the right. The antagonist affinities were reported as pK_B estimates (Table 1, Fig. 4). Compounds **20a** and **21a** at higher concentrations depressed the maximum effect of phenylephrine. Reduction of phenylephrine maxima indicates a more complex interaction between the tested compounds, α_1-adrenoceptors and probably other receptor systems present in the rat aorta which limits the maximal effect of phenylephrine. Other possibilities include a slow dissociation of the agent from a receptor and an allosteric modification of receptors.[30]

Compound **20a** displayed an ability to block the contractions induced by phenylephrine and it shifted the phenylephrine response to the right giving a pK_B estimate of 7.785 ± 0.025. Compound **21a** also shifted the phenylephrine response to the right indicating an interaction with α_1-adrenoceptors present in rat aorta. The pK_B value was 7.441 ± 0.025. It is noticeable that the affinity from the functional test for compounds **20a** and **21a** was in the same concentration range as determined at radioligand binding assay.

2.3. Molecular modelling study

The goal of our molecular modelling was to search for 3D-structure properties of arylpiperazine derivatives (**9a**–**22a**), responsible for discrimination between α_1-adrenoceptors and 5-HT_{1A} receptors. The studies are based on two pharmacophore models: the Barbaro's[18] model for α_1-adrenoceptor antagonists and Lepailleur's[26] model for ligands of 5-HT_{1A} receptors. The calculations performed previously[27] were modified using newer, more precise methods.[31–38] The lowest energy conformation for each compound was found (Fig. 6) and considered as the bioactive one. In case of **9a**–**11a**, **15a**–**18a**, **22a**, substituted at N3 position of the hydantoin ring with longer fragments (ethyl, ester, acetic acid), the substituent places perpendicularly to the plane of the imidazole ring,

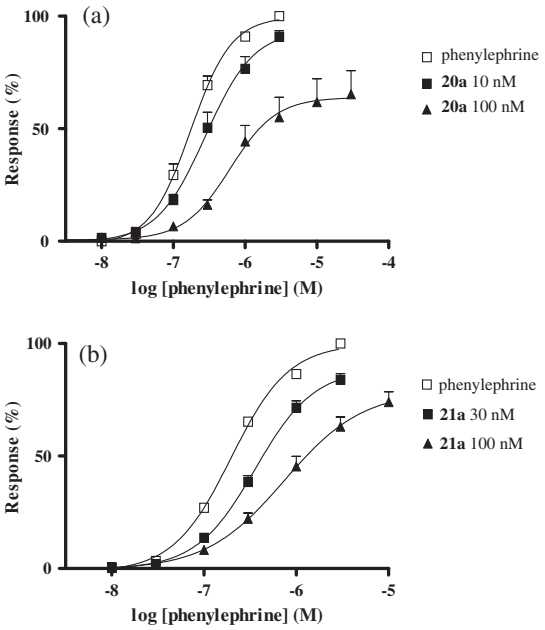

Figure 4. Concentration–response curves to phenylephrine in the rat aorta in the absence (□) or presence of (a) **20a** (■ 10 and ▲ 100 nM); (b) **21a** (■ 30 and ▲ 100 nM). Results are expressed as percentage of the maximal response to phenylephrine in the first concentration–response curve. Each point represents the mean ± SEM (n = 4).

directing mostly towards piperazine. Compound **10a** has the ester fragment directed outside the molecule (Fig. 5)—as a matter of fact, similar conformations have been also found for other structures with longer N3 substituents as energetic local minima; their potential energy was not higher than 2 kJ/mol over global minimum. In all presented conformations internal hydrogen bonds have been found: between the hydroxy group and the carbonyl in the position 2 of hydantoin ring (**9a**–**13a**, **15a**–**22a**) or between the protonated piperazine nitrogen N4 and the acetyl oxygen (**14**). Results of calculated spatial properties in the comparison to both Barbaro's and Lepailleur's pharmacophore models are shown in Figure 7. Properties of substituents at nitrogen N3 for selected compounds with different pharmacological activities (**10a**, **13a**, **20a** and **22a**) are displayed in Figure 8.

Concerning Barbaro's model, the computed results indicated a high spatial similarity of the compounds **9a**–**22a** in the area of two pharmacophoric features, PI-HY1 (X1) and PI-HY2 (X2). In case of the distance X1 between a positive ionisable centre PI and a hydrophobic area HY1 (Fig. 7a), the values in range of 5.68–5.69 Å are almost identical with the one described for the

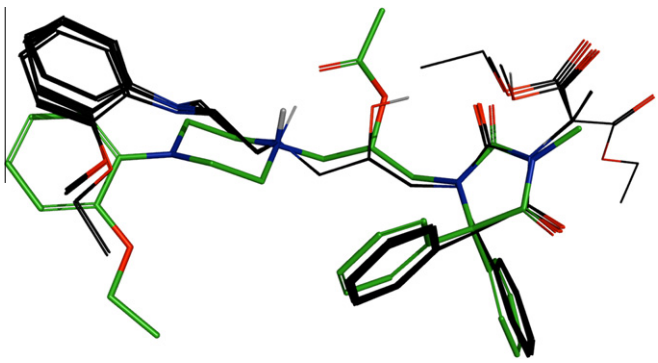

Figure 5. Molecular modelling results. Superimposition of global energy minimum conformations of **9a**–**22a** after molecular mechanics conformational analysis. Non polar hydrogens are not displayed. Conformation of **14** is coloured green.

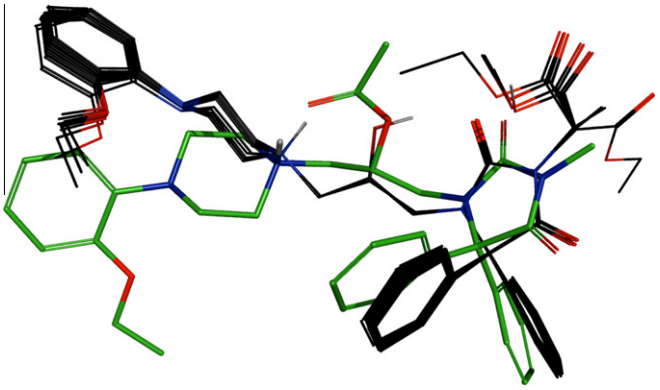

Figure 6. Molecular modelling results. Superimposition of global energy minimum conformations of **9a**–**22a** after reoptimization (DFT) calculations. Non polar hydrogens are not displayed. Conformation of **14** is coloured green.

pharmacophore model. Similarly, the calculated distance PI-HY2 (X2) fits almost perfectly in the pharmacophore model, placing in the narrow range of 6.18–6.20 Å for the compounds **10a**–**18a** and **20a**–**22a**. The calculated distance PI-HBA (X3) is in similar range (5.11–5.15 Å) for all 2-hydroxypropyl derivatives (**9a**–**13a** and **15a**–**22a**), lower than that of Barbaro's model in 8–9%. On the other hand, in case of acetoxy derivative **14a**, the X3 value is 6.8% higher than the one given by Barbaro. The distance between the positive ionisable centre and the centre of most peripheral aromatic ring HY3 (X4) was computed as distinctly lower than that of the pharmacophore model of Barbaro (9.78 Å), in range of 7.95–8.08 Å for 2-hydroxypropyl derivatives (**9a**–**13a** and **15a**–**22a**) and in the value of 7.60 Å for the compound **14a**.

As Lepailleur's pharmacophore features (Fig. 3), six following distances were considered: between hydrophobic area HYD and hydrogen bound acceptor HBA (Y1), HBA and aromatic ring AR (Y2); HBA and positive ionisable centre PI (Y3), HYD and AR (Y4), HYD and PI (Y5) and between PI and AR (Y6).[26] Results of the molecular modelling study (Fig. 7b) indicate a high convergence only in case of distances Y6 for all investigated compounds (**9a**–**22a**). The compounds display values of distance Y1 in range of 5.53–5.62 Å, significantly higher than the pharmacophoric one (4.4 Å). In case of distances Y2–Y5, a decrease, in comparison with an ideal Lepailleur's pharmacophoric features, can be observed. All 2-hydroxypropyl derivatives show approximately 17% shortening of distance Y2 (10.08–10.23 Å) in comparison with that of Lepailleur's model (12.2 Å), whereas a much better accordance is seen for acetoxy derivative **14a** (11.68 Å). Similarly, compounds **9a**–**13a** and **15a**–**19a** have distance Y3 in range of 5.11–5.15 Å while this distance for compound **14a** (6.0 Å) is closer to that of pharmacophore model (6.6 Å). The distances Y4 are approximately 2 Å shorter than the pharmacophoric one (15.8 Å) for 2-hydroxypropyl derivatives (13.65–13.69 Å) and almost 3.5 Å shorter for compound **14a** (12.24 Å). The molecular modelling calculations gave distances HYD-PI (Y5) in range of 7.95–8.08 Å for 2-hydroxypropyl derivatives and 7.6 Å for 2-acetoxypropyl derivative **14a**, which is clearly lower than the Y5-distance of 5-HT_{1A} pharmacophore model (10.2 Å).

2.4. SAR-study

As a continuation of previously started study,[2,27] the presented modifications were focused on the substituent at N3-position of hydantoin. The performed synthesis allowed to save free NH at position N3 (**19a**–**21a**) as well as deprotect previously obtained ester giving carboxylic end (**22a**). Results of affinity for both α_1-AR and 5-HT_{1A} receptors, determined for previously (**9a**–**18a**) and currently obtained compounds (**19a**–**22a**), showed the role of the modified fragment for the biological activities (Table 1). In case of activity at 5-HT_{1A}, three classes of activity may be observed (I–III). Within the series of 2-alkoxyphenylpiperazine derivatives ($R^2 = OCH_3$, OC_2H_5) compounds substituted at N3 with methyl group (**12a**–**14a**), 2-methyl-propionic ester (**11a** and **18a**) and acetic acid ester (**16a**) belong to the class of the most potent ligands (class I), while esters (**10a**, **15a** and **17a**) as well as N3H-free derivatives (**20a** and **21a**) represent the class of active ligands (class II). In the group of moderate activity (class III), compounds with unsubstituted phenylpiperazine phenyl ring (R^2 = H, **9a**, **19a**) and with N3-acetic acid end (**22a**) can be found.

On the other hand, the presence of carboxylic moiety at N3 position critically decreased affinity for α_1-adrenoceptors, what is observed in case of compound **22a** (K_i = 4800 nM) in comparison to the corresponding ester **10a** (K_i = 160 nM). The conserved NH group at N3-position (**20a** and **21a**, Table 1) improved affinity for α_1-adrenoceptors of corresponding N3-substituted hydantoin **9a**–**18a** (Table 1).[27]

The pharmacological studies performed for arylpiperazine hydantoin derivatives **9a**–**22a** indicated that most of the tested compounds (**10a**–**16a**, **18a**, **19a** and **22a**) acted stronger on 5-HT_{1A} than on α_1-adrenergic receptors (Table 1). The significantly higher activity toward α_1-AR comparing to 5-HT_{1A} was observed only in case of 1-(2-hydroxy-3-(4-(2-methoxyphenyl)piperazin-1-yl)propyl)-5,5-diphenylimidazolidine-2,4-dione hydrochloride (**20a**), a compound with NH-free at position 3 of hydantoin. In case of compounds with unsubstituted phenylpiperazine phenyl ring (**9a**, **19a**) as well as 2-methoxyphenylpiperazine derivative with methyl 2-propionate end (**17a**), the affinity values for both, 5-HT_{1A} and α_1-adrenergic receptors, are comparable. According to the binding assays results (Table 1), unsubstituted phenylpiperazine phenyl ring (**9a**, **19a**) is less profitable for both 5-HT_{1A} and α_1-adrenergic receptors affinities. In case of affinity for α_1-adrenoceptors, the decrease of activity may be explained basing on the pharmacophore model of Barbaro,[18] as the unsubstituted phenylpiperazine derivatives do not include pharmacophore feature HY2, desirable for α_1-AR-antagonistic properties (Fig. 3). The Lepailleur model for 5-HT_{1A} receptor ligand[26] does not respect this structural feature as necessary for the activity (Fig. 3), however, our results demonstrated a significant influence of this feature on the affinity for 5-HT_{1A} receptors.

Generally, the introduction of an alkyl-5,5-diphenylhydantoin fragment at phenylpiperazine[2,27] seems to be profitable for the affinity for 5-HT_{1A} but this is limited by N3-substitution. N3-methyl (**12a**) and N3-ethyl propionate substituents are the most profitable (**11a**) as they increased the 5-HT_{1A} affinity of corresponding free 2-methoxyphenylpiperazine (K_i = 68 nM).[13] The following order of activity for N3-substituents can be observed: methyl > ethyl propionate > methyl 2-propionate > H > ethyl acetate > methyl acetate > acetic acid (Table 1). The highest decrease of affinity for 5-HT_{1A} (approximately 10-fold) is observed when 2-methoxyphenylpiperazine is linked to DPH with N3-acetic acid end (**22a**). However, the acidic end of the compound **22a** seems to be much more disadvantageous for activity at α_1-AR (Table 1). The compound **22a** displayed almost 30-fold decrease of activity of its corresponding esters (**10a**, **15a**). Our results also demonstrated that the 2-ethoxyphenylpiperazine fragment is more profitable for 5-HT_{1A} affinity than the 2-methoxyphenylpiperazine one. Comparing four pairs of corresponding 2-ethoxy- and 2-methoxyphenylpiperazine derivatives (**13a**–**12a**, **16a**–**15a**, **18a**–**17a** and **21a**–**20a**), it can be concluded that the 2-ethoxyphenylpiperazine derivative was more active in each pair (Table 1). An analysis of an influence of an alkyl spacer on affinity for both 5-HT_{1A} and α_1-AR indicated that the acetoxy substituent at the alkyl chain linking piperazine to hydantoin fragment caused fivefold decrease

(a) Structural factors responsible for α_1-AR binding

(b) Structural factors responsible for 5 -HT_{1A} binding

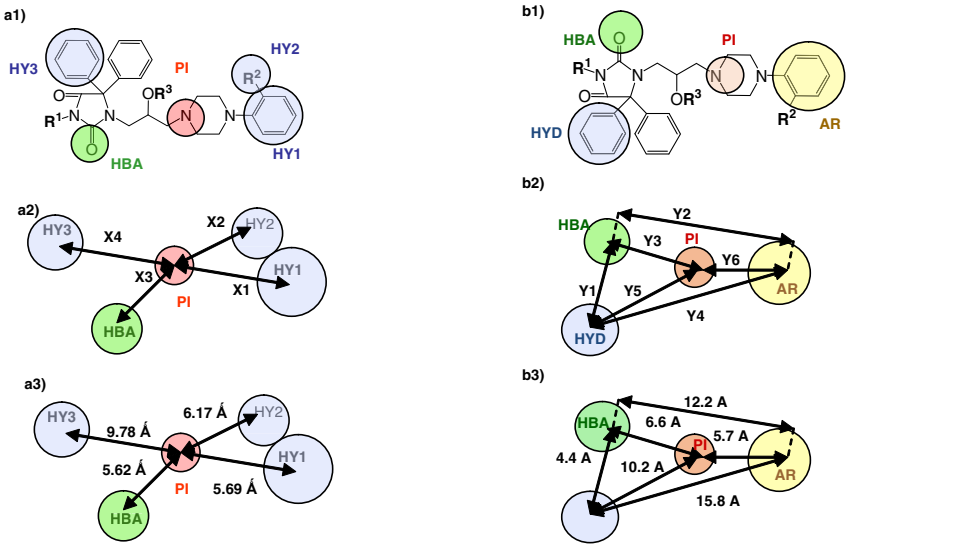

Cpd	X1=Y6 [Å]	X2[Å]	X3=Y3[Å]	X4=Y5[Å]	Y1[Å]	Y2[Å]	Y4[Å]
9a	5.68	-	5.13	8.05	5.62	10.08	13.71
10a	5.68	6.19	5.14	8.05	5.57	10.16	13.66
11a	5.68	6.18	5.15	8.05	5.58	10.22	13.65
12a	5.68	6.18	5.13	7.95	5.61	10.16	13.69
13a	5.68	6.19	5.12	8.08	5.62	10.14	13.71
14a	5.69	6.20	6.00	7.60	5.53	11.68	12.24
15a	5.68	6.18	5.13	8.05	5.59	10.17	13.69
16a	5.69	6.19	5.14	8.04	5.62	10.17	13.91
17a	5.69	6.20	5.12	8.02	5.58	10.13	13.68
18a	5.69	6.18	5.14	8.02	5.55	10.18	13.65
19a	5.69	-	5.11	8.06	5.62	10.08	13.71
20a	5.69	6.19	5.12	8.06	5.62	10.13	13.70
21a	5.69	6.19	5.13	8.07	5.62	10.13	13.71
22a	5.69	6.20	5.13	8.05	5.59	10.23	13.70

Figure 7. Structural parameters of compounds **9a**–**22a** in the comparison with two pharmacophore models. Distances corresponding with both, Barbaro's and Lepailleur's models, according to the molecular modelling calculation for compounds **9a**–**22a** (below the pictures). (a) Barbaro's model for α_1-adrenoceptor antagonists; (a1) five pharmacophore features mapped by phenylpiperazine derivatives of phenytoin; (a2) four distances affect binding properties at α_1-adrenoceptor; X1(PI-HY1), X2 (PI-HY2), X3 (PI-HBA) and X4 (PI-HY3); (a3) distances X1-X4 for ideal a1-AR antagonist. (b) Lepailleur's model for 5-HT_{1A} receptor ligands; (b1) four pharmacophore features mapped by phenylpiperazine derivatives of phenytoin; (b2) six distances affect binding properties at 5–HT_{1A} receptor; Y1(HYD-HBA), Y2 (AR-HBA), Y3 (PI-HBA), Y4 (HYD-AR), Y5 (PI-HYD) and Y6 (PI-AR); (b3) distances Y1–Y6 for ideal 5-HT_{1A} ligand.

of the affinity for both receptors (compounds **13a** and **14a**, Table 1).

The results of the pharmacological assays exhibited that most of modifications performed for compound **AZ–99** (**9a**)[2,27] resulted in compounds with higher activity at 5-HT_{1A} than that of α_1-AR. However, the pharmacophore-based SAR analysis did not confirm this conclusion. Compounds **9a**–**22a** displayed a significantly higher accordance with Barbaro's pharmacophore features, dedicated to α_1-adrenoceptor antagonists, than with Lepailleur's model for 5-HT_{1A} ligands. The compounds **9a**–**22a** possess all structural fragments characteristic for both, Barbaro's and Lepailleur's models, but some divergence in the features collocation is observed (Fig. 7). As Barbaro's model is concerned, all compounds (**9a**–**22a**) display high accordance with the ideal antagonist behaviour within the areas of HY1, PI and HY2 (**10a**–**18a**, **20a**–**22a**). Differences in the distances PI-HBA (X3) for compounds **9a**–**22a** are lower than 10% in comparison to the ideal antagonist. The shortening of X3-distance is observed for all compounds with a hydroxypropyl linker, while a little prolongation for 2-acetoxypropyl derivative **14a** can be seen. Similarly, all compounds **9a**–**22a** exhibit some deviation in the location of the third hydrophobic feature (HY3). There are two aromatic rings present in the non-phenylpiperazine area, but each of them is located too close to the positive ionisable nitrogen (PI) comparing to the ideal distance described by Barbaro (Fig. 7). Although the most distant aromatic ring was considered as the HY3-area for each compound (**9a**–**22a**), the distances between the HY3 centre and PI are shorter (17–19%) for 2-hydroxypropyl derivatives (**9a**–**13a**, **15a**–**22a**) and, particularly, for 2-acetoxypropyl derivative **14a** (22.3%). These differences may explain a decrease of α_1-adrenoceptors affinity for compound **14a** comparing to the corresponding 2-hydroxypropyl derivative (**13a**).[27]

The presented group of arylpiperazine derivatives **9a**–**22a** exhibits also a good agreement with a previously described α_1-AR antagonist pharmacophore model of De Benedetti[15] which requires a presence of protonated nitrogen (P) and two aromatic systems (Ar1, Ar2) located 4–7 Å from P (Fig. 2). Within the group of compounds **9a**–**22a** a distance from the positive ionisable nitrogen PI to the centre of phenylpiperazine phenyl ring HY1

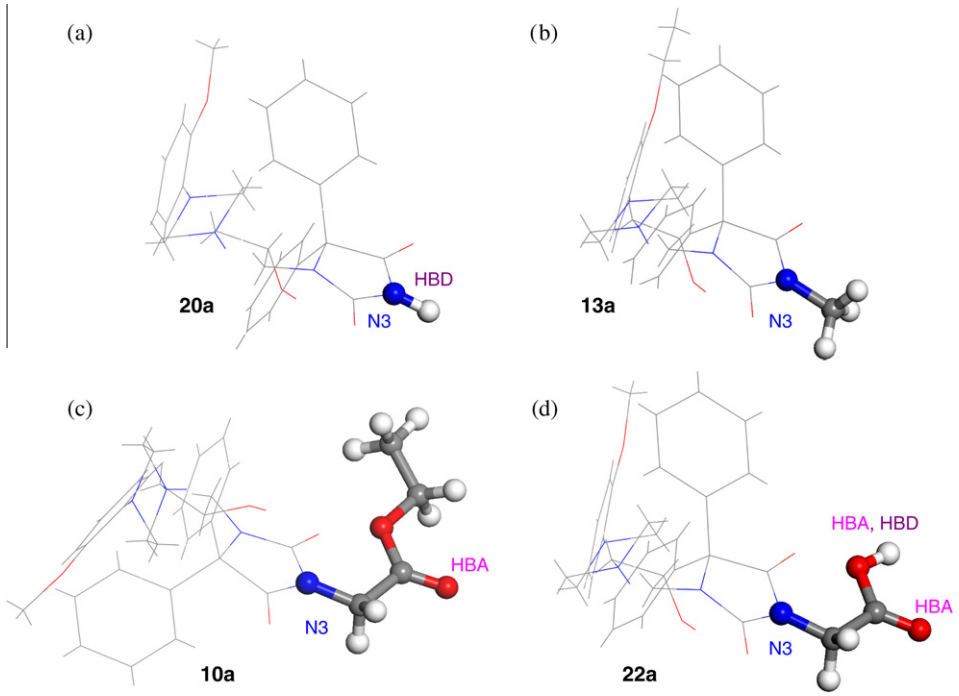

Figure 8. Properties of substituents at nitrogen N3 for selected arylpiperazine derivatives of hydantoin with different pharmacological activity; HBA-hydrogen bond acceptor site; HBD-hydrogen bond donor site. (a) N–H, the strongest α_1-AR agent **20a**. (b) N–CH_3, the strongest 5-HT_{1A} agent **13a**. (c) N–$CH_2COOC_2H_5$, a long ester N3-substituent of **10a**, a compound active for both receptors. (d) N–CH_2COOH, acid substituent of compound **22a** displaying a noticeable decrease of activity for both, α_1-AR and 5-HT_{1A}, receptors.

(5.68–5.69 Å, Fig. 7a) fits in De Benedetti's distance P-Ar1. De Benedetti's feature Ar2 can match the closer hydantoin phenyl ring, which is placed 4.98 Å from protonated nitrogen for the compound **14a** and 5.58–6.16 Å for the rest of compounds (**9a**–**13a** and **15a**–**22a**). In both cases, the considered distances are between 4 Å and 7 Å—in agreement with Benedetti's pharmacophore requirements.

On the other hand, it is hard to explain differences in 5-HT_{1A} affinity for compounds **9a**–**22a** basing on the pharmacophore model of Lepailleur. The analysis of the Lepailleur's pharmacophore features collocation for an ideal 5-HT_{1A} ligand (Fig. 7b) demonstrates that the hydantoin derivatives **9a**–**22a** match the model only within one out of six crucial distances (Y6). In case of distance Y1, hydrophobic centre and hydrogen bond acceptor are located 26–28% too far in comparison to the pharmacophore model distance. In case of distances Y2–Y5, the target pharmacophore features are located too close, giving a shortening of the following distances for compounds with hydroxypropyl linker: Y2 (17%), Y3 (23%), Y4 (13%) and Y5 (22%). A different behaviour can be noticed for acetoxy derivative **14a**, which demonstrated a higher accordance with the pharmacophore model within the distances Y2 (4.3% shortening) and Y3 (9% shortening), whereas its deviations from the distances HYD-AR (Y4) and HYD-PI (Y5) were significantly higher, that is, 22% (Y4) and 25% (Y5). SAR-studies based on a simple pharmacophore model for buspiron-like 5-HT_{1A} receptor ligands, described by Chilmonczyk et al.,[13,25] gave similar inferences. Compounds **9a**–**22a** show significant deviations (13–43%) from the ideal distances d_1–d_3 (Fig. 2).

The tested compounds **9a**–**22a** showed various α_1/5-HT_{1A} selectivity values (Table 1) in range of 0.17–17.37. The most selective compounds (**13a**, **14a**) belong to the N3-methyl derivatives of hydantoin with 2-ethoxyphenylpiperazine fragment. On the other hand, Betti et al.[39] described a group of 2-ethoxyphenylpiperazine derivatives of pyridazinone with explicit selectivity (1.5–119-fold) toward α_1-AR in comparison to 5-HT_{1A} receptors. The 5-HT_{1A}/α_1 selectivities for 2-methoxyphenylpiperazine pyridazinone derivatives were clearly lower. In our group of hydantoin derivatives **9a**–**22a**, a reversal behaviour can be observed (**12a**–**13a**, **15a**–**16a**, **17a**–**18a** and **20a**–**21a**). An influence of N3-ester end on the selectivity did not seem to be significant, while unsubstituted N3H fragment (**20a**, **21a**) conduced an evident increase of selectivity toward α_1-AR comparing to 5-HT_{1A} (5-HT_{1A}/α_1).

Our results indicated that compounds **9a**–**22a** showed high 3D convergence within arylpiperazine-hydantoin area (Figs. 5 and 6), covering all Barbaro's and Lepailleur's pharmacophore features, nevertheless their affinity and selectivity for α_1/5-HT_{1A} receptors were different. This may suggest that both pharmacophore models[18,26] are not sufficient to describe the differences in affinity and selectivity for α_1/5-HT_{1A} receptors in the group of phenylpiperazine hydantoin derivatives. Additionally, the kind of N3-substituent should be taken into consideration.

Analysis of N3-substituent properties (Fig. 8) revealed that a free NH group, the smallest fragment possessing hydrogen bond donor (HBD) properties, is especially favourable for α_1-adrenoceptors affinity (**20a**, **21a**). On the other hand, a presence of methyl group, a small H-bond-neutral substituent, placed in the neighbourhood of N3-moiety, is particularly profitable for affinity for 5-HT_{1A} receptors (**12a**–**14a**). The introduction of methyl group into N3-position deprived the compounds **20a** and **21a** of a HBD-site. A replacement of NH group with longer N-ester fragment (**10a**, **11a**, **15a**–**18a**) also removed the hydrogen bond donor site, but it increased the number of hydrogen bond acceptors (HBA) as the new C=O fragment was added. This modification seems to have rather moderate influence on the affinity and selectivity for α_1/5-HT_{1A} receptors. In the case of compound **22a**, the N3-substituent with carboxylic end can play both a role of HBD- and HBA-site. The carboxylic end seems to be a hindrance in the interaction with both, 5-HT_{1A} and α_1-adrenergic receptors as this modification

decreased affinity of corresponding esters (**10a**, **15a**) for 5-HT_{1A} and, particularly, for α_1-AR.

3. Conclusion

Our study performed for the group of arylpiperazine derivatives of hydantoin **9a**–**22a** provided new information in the field of structural properties responsible for affinity and selectivity toward 5-HT_{1A} receptors comparing to α_1-adrenoceptors. The molecular modelling aided SAR-analysis demonstrated the role of three following structural parameters: the substituent at phenylpiperazine phenyl ring, the substituent at the alkyl spacer and the substituent at N3-position. 2-Ethoxyphenylpiperazine moiety as well as N3-methyl substituent were particularly profitable for affinity and selectivity for 5-HT_{1A}, while 2-methoxyphenylpiperazine fragment and free N3H group were preferable for α_1-AR. Phenylpiperazine moiety with the unsubstituted phenyl ring, the N3-acetic acid end or acetoxy substituent at the alkyl spacer were unfavourable for affinity for both, 5-HT_{1A} and α_1-AR. Among considered pharmacophore models, the model of Barbaro[18] seems to be the best corresponding with the group of arylpiperazine hydantoin derivatives **9a**–**22a**. Nevertheless, none of the investigated pharmacophore models was sufficient to explain all differences in affinity and selectivity for 5-HT_{1A}/α_1-adrenoceptors among the arylpiperazine hydantoin derivatives. Our results suggest that non-pharmacophoric N3-substituent is an important factor which, according to its chemical properties, can affect affinity and discriminate between 5-HT_{1A} and α_1-adrenoceptors.

4. Experimental

4.1. Chemistry

^{1}H NMR spectra were recorded on a Varian Mercury VX 300 MHz PFG instrument (Varian Inc., Palo Alto, CA, USA) in DMSO-d_6 at ambient temperature using the solvent signal as an internal standard. IR spectra were recorded on a Jasco FT/IR-410 apparatus using KBr pellets and are reported in cm^{-1}. Thin-layer chromatography was performed on pre-coated Merck silica gel 60 F_{254} aluminium sheets, the used solvent systems were: (I) toluene/acetone 40:3; (II) toluene/acetone/methanol 5:5:1; (III) methanol/dichloromethane 7:1. Melting points were determined using Mel-Temp II apparatus and are uncorrected. Elemental analyses were within ±0.4% of the theoretical values unless stated otherwise. Syntheses under microwave irradiation were performed in household microwave oven Samsung M1618.

4.1.1. Preparation of 5,5-diphenyl-3-tritylimidazolidine-2,4-dione (24)

A mixture of **23** (50 mmol, 12.6 g) in CH_2Cl_2 (80 mL) and TEA (100 mmol, 10 g) in CH_2Cl_2 (40 mL) was stirred in room temperature for 15 min. Trityl chloride (50 mmol, 13.9 g) in CH_2Cl_2 (300 mL) was slowly added (10 min). The reactants were mixed in room temperature for 30 h. The solution was washed with water (250 mL) and twice with diluted NaOH solution (1%, 250 mL). The organic phase was dried with anhydrous Na_2SO_4. After evaporation of the solvent, the residue was crystallized from 1-butanol giving pure white crystals of **24** (14.6 g, 29 mmol, 58%) mp 252–253 °C, R_f (I): 0.49. ^{1}H NMR for **24** (DMSO-d_6) δ (ppm): 7.03–7.08 (m, 4H, 2 × 5-Ph-3,5-H), 7.15–7.38 (m, 21H, 2 × 5-Ph-2,4,6-H, 3 × Ph_{trityl}), 9.47 (s, 1H, NH). Anal. Calcd for $C_{34}H_{26}N_2O_2$: C, 82.57; H, 5.30; N, 5.67. Found: C, 82.78; H, 5.31; N, 5.40.

4.1.2. Preparation of 1-(oxiran-2-ylmethyl)-5,5-diphenyl-3-tritylimidazolidine-2,4-dione (25)

A suspension of **24** (35 mmol, 17.29 g), K_2CO_3 (14 g), TEBA (1.05 g), in acetone (70 mL) was stirred at room temperature for 15 min, then, a solution of freshly distiled epichlorohydrin (36 mmol, 3.56 g) in acetone (42 mL) was added dropwise. The suspension was stirred for the next 54 h, then, the precipitate was removed by filtration. The solvent was evaporated. The residue was heated with CH_2Cl_2 (150 ml) under reflux for 10 min and separated from insoluble inorganic precipitate by filtration. The filtrate was evaporated and the residue was purified by crystallization from acetone/water to give bright crystals of **25** (10.6 g, 19 mmol, 53%) mp 224–226 °C, R_f (I): 0.52. ^{1}H NMR for **25** (DMSO-d_6) δ (ppm): 1.97 (dd, J_1 = 2.82 Hz, J_2 = 4.87 Hz., 1H, CH_{oxiran}), 2.26–2.30 (dd def. 2H, $CH_{2oxiran}$), 2.02–3.09 (dd def., 1H, N1-CH_{2a}), 3.24–3.28 (m, 1H, N1-CH_{2b}), 6.90–7.46 (m, 25H, 5 × Ph). Anal. Calcd for $C_{37}H_{30}N_2O_3 \times 0.5\ H_2O$: C, 76.93; H, 5.76; N, 4.85. Found: C, 76.40; H, 5.49; N, 4.70.

4.1.3. General procedure for preparation of 1-(2-hydroxy-3-(4-arylpiperazin-1-yl)propyl)-5,5-diphenyl-3-tritylimidazolidine-2,4-diones (26–28)

Equimolar (5–6 mmol) amounts of appropriate arylpiperazine and 1-(oxiran-2-ylmethyl)-5,5-diphenyl-3-tritylimidazolidine-2,4-dione (**25**) were dissolved in CH_2Cl_2 (20–30 ml) in a flat-bottomed flask and mixed for 2 min. The solvent was evaporated, then, the residue was irradiated in a standard household microwave oven using various powers (450–600 W) and times (7–25 min) of irradiation for each prepared compound, respectively. The progress of reaction was controlled with TLC (II). After irradiation, the glassy residue was heated with methanol (15–20 ml) under reflux for 30 min. During that time, the glassy residue was converted into suspension of white precipitate. The suspension was left at 0–4 °C overnight. The precipitate was filtrated to give ready compounds **26**–**28**.

4.1.3.1. 1-(2-Hydroxy-3-(4-phenylpiperazin-1-yl)propyl)-5,5-diphenyl-3-tritylimidazolidine-2,4-dione (26). Compound **25** (5 mmol, 2.75 g), 1-phenylpiperazine (5 mmol, 0.81 g) and 20 mL of CH_2Cl_2 were used. The irradiation: (450 W) 7 × 1 min. The purification from 15 ml of methanol was performed. White crystals of **26** (2.8 g, 3.9 mmol, 79%) mp 186–190 °C, R_f (II):0.86. ^{1}H NMR for **26** (DMSO-d_6) δ (ppm): 1.78–1.99 (m, 2H, Pp-CH_2), 2.11–2.14 (t def., 4H, Pp-2,6-H), 2.80–2.89 (m, 1H, C*H*OH), 2.89–2.94 (t def., 4H, Pp-3,5-H), 3.08–3.11 (d def., 2H, N1-CH_2), 3.25–3.60 (m, 1H, OH), 6.72 (t, J = 7.31 Hz, 1H, PpPh-4-H), 6.86–7.45 (m, 29H, PpPh-2,3,5,6-H, 5 × Ph). Anal. Calcd for $C_{47}H_{44}N_4O_3$: C, 79.19; H, 6.22; N, 7.86. Found: C, 79.26; H, 6.20; N, 7.82.

4.1.3.2. 1-(2-Hydroxy-3-(4-(2-methoxyphenyl)piperazin-1-yl)-propyl)-5,5-diphenyl-3-tritylimidazolidine-2,4-dione (27). Compound **25** (6 mmol, 3.30 g), 1-(2-methoxyphenyl)piperazine (6 mmol, 1.15 g) and 30 mL of CH_2Cl_2 were used. The irradiation: (450 W) for 15 min (3 × 1 min and 8 × 1.5 min). The purification from 20 ml of methanol was performed. White crystals of **27** (4.1 g , 5.5 mmol, 92%) mp 188–192 °C, R_f (II):0.79. ^{1}H NMR for **27** (DMSO-d_6) δ (ppm): 1.83–1.98 (m, 2H, Pp-CH_2), 2.14 (br s, 4H, Pp-2,6-H), 2.77 (br s, 4H, Pp-3,5-H), 2.90–3.02 (m, 1H, C*H*OH), 3.06–3.12 (m, 2H, N1-CH_2), 3.76 (s, 3H, OCH_3), 4.38 (d, J = 4.88 Hz, 1H, OH), 6.82–7.43 (m, 29H, PpPh, 5 × Ph). Anal. Calcd for $C_{48}H_{46}N_4O_4$: C, 77.60; H, 6.24; N, 7.54. Found: C, 77.48; H, 6.27; N, 7.51.

4.1.3.3. 1-(3-(4-(2-Ethoxyphenyl)piperazin-1-yl)-2-hydroxypropyl)-5,5-diphenyl-3-tritylimidazolidine-2,4-dione (28). Compound **25** (5 mmol, 2.75 g), 1-(2-ethoxyphenyl)piperazine (5 mmol, 1.03 g) and 20 mL of CH_2Cl_2 were used. The irradiation:

450 W for 4 min (4 × 1 min), then (600 W) for 21 min (3 × 1 min and 9 × 2 min). The purification from 15 ml of methanol was performed. White crystals of **28** (2.5 g, 3.3 mmol, 66%) mp 190–194 °C, R_f (II):0.84. ^{1}H NMR for **28** (DMSO-d_6) δ (ppm): 1.33 (t, J = 7.08 Hz, 3H, OCH_2CH_3), 1.80–1.93 (m, 2H, Pp-CH_2), 2.13 (br s, 4H, Pp-2,6-H), 2.80 (br s, 4H, Pp-3,5-H), 2.85–2.95 (m, 1H, C*H*OH), 3.09 (d, J = 6.67 Hz, 2H, N1-CH_2), 3.96 (q, J = 6.97 Hz, 2H, OCH_2CH_3), 4.40 (br s, 1H, OH), 6.78–6.95 (m, 4H, PpPh), 7.06–7.45 (m, 25H, 5 × Ph). Anal. Calcd for $C_{49}H_{48}N_4O_4$: C, 77.75; H, 6.39; N, 7.40. Found: C, 77.77; H, 6.38; N, 7.38.

4.1.4. General procedure for preparation of 1-(2-hydroxy-3-(4-arylpiperazin-1-yl)propyl)-5,5-diphenylimidazolidine-2,4-dione hydrochlorides (19a–21a)

1-(2-Hydroxy-3-(4-arylpiperazin-1-yl)propyl)-5,5-diphenyl-3-tritylimidazolidine-2,4-dione (**26**–**28**) (1.32–1.4 mmol, 1 g) was dissolved in CH_2Cl_2 (10 ml) by an intensive stirring for 5–10 min. A water solution of TFA (90%, 10 mL) was added. The mixture was stirred at room temperature for 18–20 h. Then, the solution was twice washed with water (2 × 30 mL). The organic phase was dried with anhydrous potassium carbonate. The solution was condensed by evaporation of CH_2Cl_2 and purified by column chromatography using silica gel and dichloromethane: acetone (10:1)/MeOH as eluents to give a compound (**19**–**21**) as a bright oil. The oil was dissolved in methanol and was saturated with dried gaseous hydrogen chloride until acidic pH. The pure crystals of a desirable hydrochloride were obtained after cooling at 0–4 °C overnight (**19a**) or were precipitated with diethyl ether (**20a** and **21a**).

4.1.4.1. 1-(2-Hydroxy-3-(4-phenylpiperazin-1-yl)propyl)-5,5-diphenylimidazolidine-2,4-dione hydrochloride (19a).

1-(2-Hydroxy-3-(4-phenylpiperazin-1-yl)propyl)-5,5-diphenyl-3-tritylimidazolidine-2,4-dione **26** (1.4 mmol, 1 g) was stirred with TFA for 18 h. The pure **19a** was precipitated from methanol to give bright-pink powder (0.14 g, 0.26 mmol, 18%) mp 250–252 °C, R_f (II): 0.67. ^{1}H NMR for **19a** (DMSO-d_6) δ (ppm): 2.61–2.68 (t def., 1H, C*H*OH), 2.76–2.82 (m, 2H, Pp-CH_2), 2.93–3.11 (m, 4H, Pp-2,6-H), 3.14–3.40 (m, 4H, Pp-3,5-H), 3.66–3.70 (m, 2H, N1-CH_2), 5.88 (br s, 5H, CHO*H*, H_2O), 6.81 (t, J = 7.31 Hz, 1H, PpPh-4-H), 6.94 (d, J = 7.69 Hz, 2H, PpPh-2,6-H), 7.21–7.30 (m, 6H, 2 × Ph-2,4,6-H), 7.41–7.49 (m, 6H, 2 × Ph-3,5-H, PpPh-3,5-H), 10.13 (br s, 1H, NH^+), 11.46 (s, 1H, N3-H). IR (KBr) (cm^{-1}): 3266 (OH), 3062 (N3-H), 3002 (CH), 2485 (NH^+), 1765 (C2═O), 1716 (C4═O), 1594 (Ar). Anal. Calcd for $C_{28}H_{30}N_4O_3 \times HCl \times 1.6\ H_2O \times 0.1\ CH_2Cl_2$: C, 61.89; H, 6.42; N, 10.31. Found: C, 62.06; H, 6.47; N, 10.27.

4.1.4.2. 1-(2-Hydroxy-3-(4-(2-methoxyphenyl)piperazin-1-yl)propyl)-5,5-diphenylimidazolidine-2,4-dione hydrochloride (20a).

1-(2-Hydroxy-3-(4-(2-methoxyphenyl)piperazin-1-yl)propyl)-5,5-diphenyl-3-tritylimidazolidine-2,4-dione **27** (1.35 mmol, 1 g) was stirred with TFA for 18 h. The pure **20a** was precipitated from methanol/diethyl ether to give white powder (0.26 g, 0.46 mmol, 34%) mp 240–242 °C, R_f (II): 0.65.^{1}H NMR for **20** (DMSO-d_6) δ (ppm): 1.97–1.99 (m, 2H, Pp-CH_2), 2.19 (br s, 4H, Pp-2,6-H), 2.78 (br s, 4H, Pp-3,5-H), 2.96 (br s, 1H, C*H*OH), 3.22–3.28 (m, 2H, N1-CH_2), 3.73 (s, 3H, OCH_3), 4.39 (br s, 1H, OH), 6.81–6.91 (m, 4H, PpPh-3,4,5,6-H), 7.21–7.26 (m, 4H, 2 × Ph-3,5-H), 7.43–7.46 (m, 6H, 2 × Ph-2,4,6-H, PpPh-5-H), 11.31 (br s, 1H, N3-H). Anal. Calcd for $C_{29}H_{32}N_4O_4 \times H_2O \times CH_2Cl_2$ (**20**): C, 59.70; H, 6.01; N, 9.28. Found: C, 59.34; H, 5.89; N, 9.32. ^{1}H NMR for **20a** (DMSO-d_6) δ (ppm): 2.58–2.66 (m, 1H, C*H*OH), 2.79–3.09 (m, 6H, Pp-CH_2, Pp-2,6-H), 3.27–3.48 (m, 6H, Pp-3,5-H, N1-CH_2), 3.78 (s, 3H, OCH_3), 5.15 (br s, 6H, CHO*H*, H_2O, CH_2Cl_2), 6.87–6.88 (m, 2H, PpPh-4,6-H), 6.94–7.03 (m, 2H, 2 × Ph-4-H), 7.22–7.31 (m, 4H, 2 × Ph-2,6-H), 7.43–7.51 (m, 6H, 2 × Ph-3,5-H, PpPh-3,5-H), 9.82 (br s, 1H, NH^+), 11.44 (s, 1H, N3-H). IR (KBr) (cm^{-1}): 3268 (OH), 3062 (N3-H), 3004 (CH), 2484 (NH^+), 1764 (C2═O), 1715 (C4═O), 1595(Ar). Anal. Calcd for $C_{29}H_{32}N_4O_4 \times HCl \times 1.4\ H_2O \times CH_2Cl_2$ (**20a**): C, 61.62; H, 6.33; N, 9.88. Found: C, 62.12; H, 6.35; N, 10.00.

4.1.4.3. 1-(3-(4-(2-Ethoxyphenyl)piperazin-1-yl)-2-hydroxypropyl)-5,5-diphenylimidazolidine-2,4-dione hydrochloride (21a).

1-(3-(4-(2-Ethoxyphenyl)piperazin-1-yl)-2-hydroxypropyl)-5,5-diphenyl-3-tritylimidazolidine-2,4-dione **28** (1.32 mmol, 1 g) was stirred with TFA for 20 h. The pure **21a** was precipitated from methanol/diethyl ether to give white powder (0.30 g , 0.55 mmol, 42%) mp 234–236 °C, R_f (II): 0.63. ^{1}H NMR for **21** (DMSO-d_6) δ (ppm): 1.29 (t, J = 7.05 Hz, 3H, OCH_2CH_3), 2.02–2.32 (d def., 6H, Pp-CH_2, Pp-2,6-H), 2.71–2.96 (m, 5H, Pp-3,5-H, C*H*OH), 3.24–3.33 (m, 2H, N1-CH_2), 3.93 (q, J = 6.92 Hz, 2H, OCH_2CH_3), 4.43 (d, J = 5.13 Hz, 1H, OH) 6.80–6.88 (m, 4H, PpPh-4,6-H, 2 × Ph-4-H), 7.12–7.26 (m, 4H, 2 × Ph-2,6-H), 7.42–7.48 (m, 6H, 2 × Ph-3,5-H, PpPh-3,5-H), 11.33 (br s, 1H, N3-H). Anal. Calcd for $C_{30}H_{34}N_4O_4 \times CH_2Cl_2 \times 0.5\ H_2O$ (**21**): C, 61.18; H, 6.13; N, 9.21. Found: C, 60.94; H, 6.21; N, 9.11. ^{1}H NMR for **21a** (DMSO-d_6) δ (ppm): 1.35 (t, J = 6.92 Hz, 3H, OCH_2CH_3), 2.63–2.71 (m, 1H, C*H*OH), 2.80–3.05 (m., 6H, Pp-CH_2, Pp-2,6-H), 3.14–3.41 (m, 6H, Pp-3,5-H, N1-CH_2), 3.98 (q, J = 6.92 Hz, 2H, OCH_2CH_3), 6.02 (br s, 5H, CHO*H*, H_2O) 6.83–7.10 (m, 4H, PpPh-4,6-H, 2 × Ph-4-H), 7.12–7.32 (m, 4H, 2 × Ph-2,6-H), 7.43–7.51 (m, 6H, 2 × Ph-3,5-H, PpPh-3,5-H), 10.09 (br s, 1H, NH^+), 11.46 (s, 1H, N3-H). IR (KBr) (cm^{-1}): 3292 (OH), 3121 (N3-H), 2971 (CH), 2430 (NH^+), 1770 (C2═O), 1720 (C4═O), 1606 (Ar). Anal. Calcd for $C_{30}H_{34}N_4O_4 \times HCl \times H_2O$ (**21a**): C, 63.32; H, 6.55; N, 9.84. Found: C, 62.98; H, 6.57; N, 9.79.

4.1.5. Preparation of 2-(3-(2-hydroxy-3-(4-(2-methoxyphenyl)-piperazin-1-yl)propyl)-2,5-dioxo-4,4-diphenylimidazolidin-1-yl)acetic acid hydrochloride (22a)

A suspension of ethyl 2-(3-(2-hydroxy-3-(4-(2-methoxyphenyl)piperazin-1-yl)propyl)-2,5-dioxo-4,4-diphenylimidazolidin-1-yl)acetate **10** (1.7 mmol, 1 g) in EtOH (5 mL) and H_2O (5 mL) was treated with KOH (8.9 mmol, 0.50 g), stirred at room temperature for 90 min, diluted with H_2O (10 mL), acidified to pH 2 (35% HCl) and evaporated. The residue was dissolved in absolute EtOH (20 ml) and saturated with gaseous HCl. Ethyl ether (20 ml) was added to precipitate a white powder of **22a** (0.56 g, 0.94 mmol, 55.4%), mp 186–187 °C, R_f (III): 0.83. ^{1}H NMR for **22a** (DMSO-d_6) δ (ppm): 2.76 (br s, 3H, Pp-CH_2, C*H*OH), 2.90–2.98 (m, 4H, Pp-2,6-CH_2), 3.34–3.40 (m, 6H, Pp-3,5-CH_2, N1-CH_2), 3.78 (s, 3H, OCH_3), 4.23 (s, 2H, N3-CH_2), 4.40–5.90 (br s, 7H, OH, H_2O) 6.87–6.94 (m, 2H, PpPh-4,6-H), 6.96–7.03 (m, 2H, PpPh-3,5-H), 7.30–7.37 (m, 4H, 2 × Ph-3,5-H), 7.46–7.48 (m, 6H, 2 × Ph-2,4,6-H), 10.06 (br s, 1H, NH^+). IR (KBr) (cm^{-1}): 3423 (OH) 3250 (OH carboxyl), 3001 (CH), 2486 (NH^+), 1768 (C2═O), 1738 (C═O carboxyl), 1710 (C4═O), 1611 (Ar). Anal. Calcd for $C_{31}H_{34}N_4O_6 \times HCl$: C, 62.57; H, 5.93; N, 9.41. Found: C, 62.44; H, 5.94; N, 9.37.

4.2. Pharmacology

4.2.1. General information

The pharmacological studies were carried out on male Wistar rats ((KRF.(WI).WU), Animal House, Faculty of Pharmacy, Jagiellonian University Medical College, Cracow) weighing 170–350 g. Treatment of laboratory animals in the present study was in full accordance with the respective Polish regulations. All procedures were conducted according to guidelines of ICLAS (International Council on Laboratory Animal Science) and approved by the Local Ethics Committee on Animal Experimentation.

Source of compounds: Phenylephrine hydrochloride, acetylcholine hydrochloride, (±)-noradrenaline hydrochloride (Sigma,

Aldrich Chemie Gmbh); Thiopental sodium (Biochemie Gmbh, Vienna); [^{3}H]-Prazosin (Amersham). Other reagents were of analytical grade from local sources.

4.2.2. Radioligand binding tests

4.2.2.1. 5-HT$_{1A}$ receptor binding assay. The in vitro affinity for native serotonin 5-HT$_{1A}$ receptors was determined by inhibiting [^{3}H]-8-OH-DPAT (170.2 Ci/mmol; PerkinElmer) binding to rat hippocampal membranes. Membrane preparation and a general assay procedure were carried out according to the previously published protocols.[29,40]

Two compound concentrations were tested: 0.1 and 1 μM, each run in triplicate. Radioactivity was determined by liquid scintillation counting in a Beckman LS 6500 apparatus. The K_S values, estimated on the basis of three independent binding experiments, were reproducible in 20%.

4.2.2.2. α$_1$-Adrenoceptor binding test. The compounds were evaluated on their affinity for α$_1$-adrenergic receptors by determining for each compound its ability to displace [^{3}H]-prazosin from specific binding sites on rat cerebral cortex. [^{3}H]-Prazosin (19.5 Ci/mmol) was used.

The tissue was homogenised in 20 vol. of ice-cold 50 mM Tris–HCl buffer (pH 7.6 at 25 °C) and centrifuged at 20,000*g* for 20 min. The cell pellet was resuspended in Tris–HCl buffer and centrifuged again. The final pellet was resuspended in Tris–HCl buffer (10 mg of wet weight/ml). 240 μl of the tissue suspension, 30 μl of [^{3}H]-prazosin and 30 μl of analysed compound were incubated at 25 °C for 30 min. To determine unspecific binding 10 μM phentolamine was used. Transfer solutions and adding reagents was performed on automated pipetting system epMotion 5070 (Eppendorf, Germany).

After incubation reaction mix was filtered immediately onto GF/B glass fibre filter mate presoaked using 96-well FilterMate Harvester (Perkin–Elmer, USA).

The radioactivity retained on the filter was counted in MicroBeta TriLux 1450 scintillation counter (Perkin–Elmer, USA). Nonlinear regression of the normalised (percent radioligand binding compared to that observed in the absence of test or reference compound—total binding) raw data representing radioligand binding was performed in GraphPad Prism 3.0 (GraphPad Software) using the built-in three parameter logistic model describing ligand competition binding to radioligand-labelled sites.

4.2.3. Functional bioassay

Isolated rat aorta was used in order to test antagonistic activity of investigated compounds for α$_1$-adrenoceptors. The male Wistar rats weighting 200–350 g were anaesthetized with thiopental sodium (75 mg/kg ip) and the aorta was dissected and placed in a Krebs-Henseleit solution and cleaned of surrounding fat tissues. The thoracic aorta was denuded of endothelium and cut into approximately 4 mm long rings. The aorta rings were incubated in 30 ml chambers filled with a Krebs–Henseleit solution (NaCl 118 mM, KCl 4.7 mM, $CaCl_2$ 2.25 mM, $MgSO_4$ 1.64 mM, KH_2PO_4 1.18 mM, $NaHCO_3$ 24.88 mM, glucose 10 mM, $C_3H_3O_3Na$ 2.2 mM, EDTA 0.05 mM) at 37 °C and pH 7.4 with constant oxygenation (O_2/CO_2, 19:1). Two stainless steel pins were inserted through the lumen of each arterial segment: one pin was attached to the bottom of the chamber and the other to an isometric FDT10-A force displacement transducer (BIOPAC Systems, Inc., COMMAT Ltd, Turkey). The aortae rings were stretched and maintained at optimal tension of 2 g and allowed to equilibrate for 2 h. The lack of endothelium was confirmed by the absence of acetylocholine (1 μM) vasorelaxant action in aortic rings precontracted by noradrenaline (0.1 μM).

Cumulative concentration–response curves to phenylephrine (0.003 to 3 μM) were obtained by the method of Van Rossum.[41] Following the first phenylephrine curve, aortae rings were incubated with tested compound (one concentration of the antagonist was used in each arterial ring in every experiment) for 20 min and the next cumulative concentration curve to phenylephrine was constructed. In order to avoid fatigue of the aortae preparation, a 60 min recovery period was allowed between phenylephrine curves.

Concentration–response curves were analysed using GraphPad Prism 4.0 software (GraphPad Software Inc., San Diego, CA, USA). Contractile responses to vasoconstrictor (in the presence or absence of tested compounds) are expressed as a percentage of the maximal phenylephrine effect (E_{max} = 100%), reached in the concentration–response curves obtained before incubation with the tested compounds. Data are the means ± SEM of four separate experiments. Schild analysis could not be performed as a result of depression of the maximal response by higher antagonist concentrations and the resulting nonparallel slopes of the concentration–response curves. The affinity was estimated with the equation pK_B = log (concentration ratio − 1) − log (molar antagonist concentration), where the concentration ratio is the ratio of equieffective agonist concentrations in the absence and in the presence of the antagonist.

4.3. Molecular modelling methods

The 3D molecule structures of **9a**–**22a** were built using Schrödinger Maestro molecular modelling environment[31] basing on the crystal structure of the (*S*)-isomer of phenylpiperazine phenytoin derivative **JH**–**9a**.[27] Basic piperazine nitrogens N4 in all structures were protonated and the charge of +1 was assigned. For each compound a conformational search was then performed using the Monte Carlo method (MCMM) as implemented in MacroModel 9.7[32] with MMFFs force field and Polak-Ribiere conjugate gradient (PRCG) options. The conformational analysis was carried out for aqueous solutions with continuum solvation treatment (Generalised Born/Solvent Accessible, GB/SA). Found global minimum energy conformations of the ligands were superimposed by a least-squares method; all heavy atoms of imidazole ring and the basic nitrogen atom N4 of piperazine were chosen as fitting points (Fig. 5). All compounds adopt an extended conformation as the global minimum energy. The geometries of the lowest energy structures obtained from the conformational analysis were finally optimised using density functional theory (DFT) and the Berny algorithm with redundant internal coordinates.[33] Becke's three-parameter B3LYP hybrid functional[34,35] and the 6-31G(d,p) basis set were applied. Harmonic vibrational frequencies were calculated for each structure to confirm the potential energy minimum. The DFT calculations were carried out using the Gaussian 03 suite of programs.[36] For the graphic presentation of selected structures (**10a**, **13a**, **20a** and **22a**), PyMOL[37] and Materials Studio v.4.4 software[38] were used.

Acknowledgements

Authors thank to Mrs. Maria Kaleta for her assistance in synthesis. Authors also thank very much Professor Andrzej J. Bojarski for his helpful suggestions concerning this study. The works were partly supported by grant K/ZDS/000727. Computing resources from Academic Computer Centre CYFRONET AGH (Grants MNiSW/SGI3700/UJ/078/2008) are gratefully acknowledged.

Supplementary data

Supplementary data associated with this article can be found, in the online version, at doi:10.1016/j.bmc.2010.11.051.

References and notes

1. Malawska, B.; Kulig, K.; Filipek, B.; Sapa, J.; Maciąg, D.; Zygmunt, M.; Antkiewicz-Michaluk, L. *Eur. J. Med. Chem.* **2002**, *37*, 183.
2. Dyląg, T.; Zygmunt, M.; Maciąg, D.; Handzlik, J.; Bednarski, M.; Filipek, B.; Kieć-Kononowicz, K. *Eur. J. Med. Chem.* **2004**, *39*, 1013.
3. Kieć-Kononowicz, K.; Stadnicka, K.; Mitka, A.; Pękala, E.; Filipek, B.; Sapa, J.; Zygmunt, M. *Eur. J. Med. Chem.* **2003**, *38*, 555.
4. Hayao, S.; Schut, R. N.; Strycker, W. G. *J. Med. Chem.* **1963**, *6*, 133.
5. Cesari, N.; Biancalani, B.; Vergelli, C.; Dal Piaz, V.; Graziano, A.; Biagini, P.; Ghelardini, C.; Galeotti, N.; Giovannoni, M. P. *J. Med. Chem.* **2006**, *49*, 7825.
6. He, H.; Richardson, J. S. *CNS Drug Rev.* **1997**, *3*, 34.
7. Cascio, G.; Manghisi, E.; Porta, R.; Foregnan, G. *J. Med. Chem.* **1985**, *28*, 815.
8. Liu, J.; He, B.; Yu, A.; Zhou, W. *Chem. Biol. Drug Des.* **2007**, *69*, 265.
9. Bohnert, J. A.; Kern, W. V. *Antimicrob. Agents Chemother.* **2005**, *49*, 849.
10. Rosini, M.; Bolognesi, M. L.; Giardina, D.; Minarini, A.; Tumiatti, V.; Melchiore, C. *Curr. Top. Med. Chem.* **2007**, *7*, 147.
11. Romeo, G.; Materia, L.; Marucci, G.; Modica, M.; Pittalá, V.; Salerno, L.; Siracusa, M. A.; Buccioni, M.; Angeli, P.; Minneman, K. P. *Bioorg. Med. Chem. Lett.* **2007**, *16*, 6200.
12. Siracusa, M. A.; Salerno, L.; Modica, M. N.; Pittala, V.; Romeo, G.; Amato, M. E.; Nowak, M.; Bojarski, A. J.; Mereghetti, I.; Cagnotto, A.; Mennini, T. *J. Med. Chem.* **2008**, *51*, 4529.
13. López-Rodríguez, M. L.; Ayala, D.; Benhamú, B.; Morcillo, M. J.; Viso, A. *Curr. Med. Chem.* **2002**, *9*, 443.
14. De Marinis, R. M.; Wise, M.; Hieble, J. P.; Ruffolo, R. R., Jr. In *The Alpha-1 Adrenergic Receptor*; Ruffolo, R. R., Jr., Ed.; Humana Press: New Jersey, 1987; pp 211–258.
15. De Benedetti, P. G.; Fanelli, F.; Menziani, M.; Cocchi, M. *J. Mol. Struct.* **1994**, *305*, 101.
16. Bremner, J. B.; Coban, B.; Griffith, R. *J. Comput. Aided Mol. Des.* **1996**, *10*, 545.
17. Bremner, J. H.; Coban, B.; Griffith, R.; Groenewoud, K. M.; Yates, B. F. *Bioorg. Med. Chem.* **2000**, *8*, 201.
18. Barbaro, R.; Betti, L.; Botta, M.; Corelli, F.; Giannaccini, G.; Maccari, L.; Manetti, F.; Strappaghetti, G.; Corsano, S. *J. Med. Chem.* **2001**, *44*, 2118.
19. Bojarski, A. J. *Curr. Med. Chem.* **2008**, *6*, 2005.
20. Hilbert, M. F.; Gittos, M. W.; Middlemiss, D. N.; Mir, A. K.; Fozard, J. R. *J. Med. Chem.* **1988**, *31*, 1087.
21. Mellin, Ch.; Vallgarda, J.; Nelson, D. L.; Björk, L.; Yu, H.; Andén, N.-E.; Csöregh, I.; Arvidsson, L.-E.; Hacksell, U. *J. Med. Chem.* **1991**, *34*, 497.
22. Van Steen, B. J.; van Wijngaarden, I.; Tulp, M. T. M.; Soudijn, W. *J. Med. Chem.* **1994**, *37*, 2761.
23. Mokrosz, M. J.; Duszyńska, B.; Bojarski, A. J.; Mokrosz, J. L. *Bioorg. Med. Chem.* **1995**, *3*, 533.
24. Gaillard, P.; Carrupt, P.-A.; Testa, B.; Schambel, P. *J. Med. Chem.* **1996**, *39*, 126.
25. Chilmonczyk, Z.; Szelejewska-Woźniakowska, A.; Cybulski, J.; Cybulski, M.; Kozioł, A. E.; Gdaniec, M. *Arch. Pharm. Pharm. Med. Chem.* **1997**, *330*, 146.
26. Lepailleur, A.; Bureau, R.; Paillet-Loilier, M.; Fabis, F.; Saettel, N.; Lemaitre, S.; Dauphin, F.; Lesnard, A.; Lancelot, J.-Ch.; Rault, S. *J. Med. Chem.* **2005**, *45*, 1075.
27. Handzlik, J.; Maciąg, D.; Kubacka, M.; Mogilski, S.; Filipek, B.; Stadnicka, K.; Kieć-Kononowicz, K. *Bioorg. Med. Chem.* **2008**, *16*, 5982.
28. Kieć-Kononowicz, K.; Zejc, A. *Pol. J. Chem.* **1984**, *58*, 761.
29. Zajdel, P.; Subra, G.; Bojarski, A. J.; Duszyńska, B.; Pawłowski, M.; Martinez, J. J. *Comb. Chem.* **2004**, *6*, 761.
30. Kenakin, T.; Jenkinson, S.; Watson, C. *J. Pharmacol. Exp. Ther.* **2006**, *319*, 710.
31. Schrödinger Suite 2009: Maestro 9.0, Schrödinger, LLC, New York, NY, 2009.
32. Schrödinger Suite 2009: MacroModel 9.7, Schrödinger, LLC, New York, NY, 2009.
33. Peng, C.; Ayala, P. Y.; Schlegel, H. B.; Frisch, M. J. *J. Comput. Chem.* **1996**, *17*, 49.
34. Becke, A. D. *J. Chem. Phys.* **1993**, *98*, 5648.
35. Stevens, P. J.; Devlin, J. F.; Chabalowski, C. F.; Frisch, M. J. *J. Phys. Chem.* **1994**, *98*, 11623.
36. Frisch, M. J.; Trucks, G. W.; Schlegel, H. B.; Scuseria, G. E.; Robb, M. A.; Cheeseman, J. R.; Montgomery, J. A. , Jr.; Vreven, T.; Kudin, K. N.; Burant, J. C.; Millam, J. M.; Iyengar, S. S.; Tomasi, J.; Barone, V.; Mennucci, B.; Cossi, M.; Scalmani, G.; Rega, N.; Petersson, G. A.; Nakatsuji, H.; Hada, M.; Ehara, M.; Toyota, K.; Fukuda, R.; Hasegawa, J.; Ishida, M.; Nakajima, T.; Honda, Y.; Kitao, O.; Nakai, H.; Klene, M.; Li, X.; Knox, J. E.; Hratchian, H. P.; Cross, J. B.; Bakken, V.; Adamo, C.; Jaramillo, J.; Gomperts, R.; Stratmann, R. E.; Yazyev, O.; Austin, A. J.; Cammi, R.; Pomelli, C.; Ochterski, J. W.; Ayala, P. Y.; Morokuma, K.; Voth, G. A.; Salvador, P.; Dannenberg, J. J.; Zakrzewski, V. G.; Dapprich, S.; Daniels, A. D.; Strain, M. C.; Farkas, O.; Malick, D. K.; Rabuck, A. D.; Raghavachari, K.; Foresman, J. B.; Ortiz, J. V.; Cui, Q.; Baboul, A. G.; Clifford, S.; Cioslowski, J.; Stefanov, B. B.; Liu, G.; Liashenko, A.; Piskorz, P.; Komaromi, I.; Martin, R. L.; Fox, D. J.; Keith, T.; Al-Laham, M. A.; Peng, C. Y.; Nanayakkara, A.; Challacombe, M.; Gill, P. M. W.; Johnson, B.; Chen, W.; Wong, M. W.; Gonzalez, C.; Pople, J. A. Gaussian 03, Revision E.01, Gaussian, Wallingford, CT, 2004.
37. PyMOL Molecular Graphics System v.0.99, DeLano Scientific.
38. Accelrys Software Inc.; Polish Country Wide Licence.
39. Betti, L.; Corelli, F.; Floridi, M.; Giannaccini, G.; Maccari, L.; Manetti, F.; Strappaghetti, G.; Botta, M. *J. Med. Chem.* **2003**, *46*, 3555.
40. Bojarski, A. J.; Cegła, M. T.; Charakchieva-Minol, S.; Mokrosz, M. J.; Maćkowiak, M.; Mokrosz, J. L. *Pharmazie* **1993**, *48*, 289–294.
41. Van Rossum, J. M. *Arch. Int. Pharmacodyn. Ther.* **1963**, *143*, 299.